BIOMOLECULES & THERAPEUTICS

Original Article
Biomol Ther 28(5), 414-422 (2020)

Fangchinoline Has an Anti-Arthritic Effect in Two Animal Models and in IL-1β-Stimulated Human FLS Cells

Thea Villa, Mijin Kim and Seikwan Oh*

Department of Molecular Medicine, School of Medicine, Ewha Womans University, Seoul 07804, Republic of Korea

Abstract

Fangchinoline (FAN) is a bisbenzylisoquinoline alkaloid that is widely known for its anti-tumor properties. The goal of this study is to examine the effects of FAN on arthritis and the possible pathways it acts on. Human fibroblast-like synovial cells (FLS), carrageenan/kaolin arthritis rat model (C/K), and collagen-induced arthritis (CIA) mice model were used to establish the efficiency of FAN in arthritis. Human FLS cells were treated with FAN (1, 2.5, 5, 10 μM) 1 h before IL-1β (10 ng/mL) stimulation. Cell viability, reactive oxygen species measurement, and western blot analysis of inflammatory mediators and the MAPK and NF-κB pathways were performed. In the animal models, after induction of arthritis, the rodents were given 10 and 30 mg/kg of FAN orally 1 h before conducting behavioral experiments such as weight distribution ratio, knee thickness measurement, squeaking score, body weight measurement, paw volume measurement, and arthritis index measurement. Rodent knee joints were also analyzed histologically through H&E staining and safranin staining. FAN decreased the production of inflammatory cytokines and ROS in human FLS cells as well as the phosphorylation of the MAPK pathway and NF-κB pathway in human FLS cells. The behavioral parameters in the C/K rat model and CIA mouse model and inflammatory signs in the histological analysis were found to be ameliorated in FAN-treated groups. Cartilage degradation in CIA mice knee joints were shown to have been suppressed by FAN. These findings suggest that fangchinoline has the potential to be a therapeutic source for the treatment of rheumatoid arthritis.

Key Words: Fangchinoline, Arthritis, Inflammation, FLS, ROS, NF-κB

INTRODUCTION

Rheumatoid arthritis (RA) is an autoimmune joint inflammatory disease which can result to pain, disability, and death (Heidari, 2011). Synovitis or inflammation of the synovial membrane, joint damage, and physical function impairment due to inflammation are hallmarks of RA. In RA, different inflammatory cells can produce the cytokines IL-1, IL-6, and TNF-α. These cytokines not only promote inflammation but also stimulate fibroblast-like synovial (FLS) cells. FLS cells have a pivotal role in the progress of rheumatoid arthritis (Bustamante *et al*., 2017). Stimulated FLS cells become activated and proliferate which will result to the hyperplasia of the synovial membrane, expression of the receptor activator of nuclear factor kappa-light-chain-enhancer of activated B cells (NF-κB) ligand which promote osteoclast activity, and production of matrix metalloproteases. These mechanisms promote bone and cartilage degradation and degraded cartilage can also produce proteases resulting in a feedback loop. Cytokines will also increase the permeability of the blood vessels and the presence of adhesion molecules which would then allow more immune cells to migrate into the joints further perpetuating chronic inflammation in the joints (Müller-Ladner *et al*., 2005).

Signaling pathways such as the NF-κB and the mitogen-activated protein kinase (MAPK) pathways have been implicated in RA. These pathways have been extensively studied and are critical in FLS activation (Simmonds and Foxwell, 2008; Thalhamer *et al*., 2008). It has been shown that the phosphorylated, activated forms of JNK, ERK, and p38 MAPKs are overexpressed in synovial tissue afflicted with RA (Schett *et al*., 2000).

Various animal models of arthritis have been designed to enable researchers to have a deeper understanding of the disease and at the same time be used for the development of novel treatments (Müller-Ladner *et al*., 2005). The carrageenan/kaolin-induced arthritis model (C/K) is a monoarthritis model that has an acute onset of 1-3 h and a plateau phase that lasts for at least 1 week (Neugebauer, 2013). Another ani-

Open Access **https://doi.org/10.4062/biomolther.2020.113**

Received Jul 3, 2020 **Revised** Jul 13, 2020 **Accepted** Jul 13, 2020
Published Online Jul 27, 2020

***Corresponding Author**
E-mail: skoh@ewha.ac.kr
Tel: +82-2-6986-6271, Fax: +82-2-6986-7014

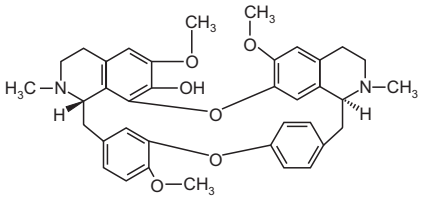

Fig. 1. Chemical structure of fangchinoline (FAN). FAN has a molecular weight of 608.7 g/mol and a molecular formula of $C_{37}H_{40}N_2O_6$. The chemical structure was drawn using ChemSketch by ACDLabs.

mal model of arthritis is the collagen-induced arthritis model (CIA). CIA has been the most studied and extensively used model of RA. This model is mainly used to understand potential pathological mechanisms of arthritis and the cells involved, as well as, designing and testing new drugs for RA (Brand *et al*., 2007).

Although a range of effective therapies for RA are available, these can only be achieved in 75 percent of patients and in those countries where these treatments are readily available (Aletaha and Smolen, 2018). Thus, there is a need to find therapeutics that can target a major driver of pathological mechanisms in RA that would be more accessible to the masses.

Phytochemicals are the basis as to how nutrient supplementation can support RA therapy. Fangchinoline (FAN) (Fig. 1) is a major alkaloid that can be extracted from the roots of *Stephaniae tetrandra*. It helps against inflammation (Choi *et al*., 2000; Hristova *et al*., 2003), and growth and proliferation of different cancer cells such as osteosarcoma cells (Li *et al*., 2017) and breast cancer cells (Wang *et al*., 2017). Not only that, FAN also has neuroprotective effects (Bao *et al*., 2019) and can protect against kidney injury in diabetic nephropathy (Jiang *et al*., 2018).

Although previous studies about FAN and its effects on inflammation and arthritis have been put forward (Shan *et al*., 2019), this study aims to investigate the functions that it possibly targets in arthritis in order to further set forth its efficacy as a potential therapeutic alternative for remedying arthritis.

MATERIALS AND METHODS

Reagents

FAN was provided by Dr. H. S. Kim, Chungbuk National University, Cheongju, Korea. Cell culture reagents were purchased from WELGENE Inc (Gyeongsan, Korea). Human IL-1β was obtained from Bio Vision Inc (Milpitas, CA, USA). Arthritis-inducing reagents were supplied by Sigma-Aldrich Co (St. Louis, MO, USA). COX-2, IL-6, and TNF-α antibodies were purchased from Santa Cruz Biotechnology (Dallas, TX, USA) and β-actin, IKKβ, IKKα, p-IKKαβ, and the total and phosphorylated forms of p38, JNK, ERK, NF-κB and IκBα antibodies were purchased from Cell Signaling Technology (Danvers, MA, USA).

In vitro experiments

Cell culture: Human FLS cells were obtained from Cell Applications, Inc (San Diego, CA, USA). Cells were cultured in 10% DMEM supplemented with 10% FBS and 1% P/S solution and incubated in 37°C with 5% CO_2. Human FLS cells were subcultured and split into a 1:4 ratio. Passages 3-6 were used. Once appropriate confluency was reached, the cells were seeded in various multi-welled culture plates for subsequent assays.

Cell viability: Human FLS cells were seeded to 1×10^4 per well in a 96-well plate. The cells were treated with FAN and stimulated after 1 h with IL-1β (10 ng/mL). 24 h after, cell viability was determined using Quanti-Max™ WST-8 assay kit (BIOMAX Co., Seoul, Korea) according to the manufacturer's protocol. The absorbance was measured at 450 nm (SpectraMax ABS Plus, Molecular Devices, San Jose, CA, USA).

Reactive oxygen species measurement: Human FLS cells were seeded to 2×10^4 cells per well in a 24-well plate. The cells were treated the same way as mentioned above. After 24 h, the conditioned medium was removed and the cells were washed twice with PBS. 1 mL of 50 μM of 7-Dichlorodihydrofluorescein diacetate (H_2DCFDA, Sigma-Aldrich Co.) solution was then added to each well. The plate was wrapped in foil and incubated for 30 min at 37°C and 5% CO_2. The fluorescence was measured at an excitation of 485 nm and emission of 530 nm (Synergy H1, BioTek Instruments Inc., Winooski, VT, USA).

Western blot: In a 6-well plate, human FLS cells were seeded at 1×10^5 cells per well. Then, the cells were treated with FAN and after 1 h, stimulated for 6 h using IL-1β (10 ng/mL). Western blot samples were prepared by lysing the cells using RIPA buffer (ELPIS Biotech Inc., Daejeon, Korea). Samples were boiled for 5 min at 100°C. 15 μg of samples were loaded in 10 and 12% SDS-PAGE gels and then transferred to a PVDF membrane. The membranes were blocked using 5% bovine serum albumin or 5% skim milk dissolved in Tris-buffered saline with 0.1% Tween-20 (TBST, Biosesang, Seongnam, Korea). After blocking, specific primary antibodies (1:1,000) were added and incubated overnight at 4°C. The membranes were washed 3 times using TBST and were incubated with secondary antibody for 2 h. After, the membranes were washed 3 times with TBST. The signals were developed using an enhanced chemiluminescence detection kit (Thermo Fisher Scientific Inc., Waltham, MA, USA).

In vivo experiments

Animals: 6-week old male DBA/1J mice (18-22 g) and 6-week old male SD rats (200-220 g) were purchased from Samtako Bio Korea (Osan, Korea). The experimental animals were given 1 week to acclimate prior to the start of the experiments. They were kept inside a cage and placed in an airconditioned room that maintain a 12 h dark/12 h light cycle with a humidity of 50 ± 10% and a temperature of 23 ± 3°C. The rodents were given *ad libitum* access to food pellets and water. The study was approved by the Institutional Animal Care and Use Committee of the College of Medicine, Ewha Womans University (Seoul, Korea). The experiments were carried out in accordance with the guidelines on the care and use of laboratory animals by the National Institute of Health and Ewha Womans University.

Carrageenan/kaolin-induced arthritis (C/K) in rats: The SD rats were divided randomly into 4 groups (n=6) as follows: non-treated non-arthritis induced group (NOR), non-treated arthritis induced group (ART), FAN-treated (10 mg/kg) arthritis induced group (ART+FAN10), and FAN-treated (30 mg/kg) arthritis induced group (ART+FAN30). On day 0, SD rats to be induced with arthritis were injected with a 5% carrageenan/ka-

olin solution (0.15 mL) in the left knee joint to induce arthritis. For 6 days following arthritis induction, FAN was administered (p.o.) to the treatment groups while NOR and ART received saline 1 h before conducting behavioral assessments such as weight distribution ratio, knee thickness measurement, and squeaking score. The weight distribution ratio was measured using an incapacitance meter (Ugo Basile Biological Research Apparatus Company, Comeria-Varese, Italy) in order to estimate the amount of force the rats were using on each hind paw. The pain-bearing paw would bear lesser force than the unaffected paw. The knee thickness was measured with the use of an electronic Vernier caliper and the squeaking score was measured by counting the total number of squeakings the rats made after every flexion and extension done to the affected knee every 5 s for 10 times.

Collagen-induced arthritis (CIA) in mice: The mice were divided into four groups (n=6) that parallels the C/K model. On day 0, DBA/1J mice were injected at the base of the tail intradermally with a 50 μL solution composed of acetic acid dissolved type II collagen solution in complete Freund's adjuvant. After 14 days, a booster dose was given consisting of acetic acid dissolved type II collagen solution in incomplete Freund's adjuvant. A day after the booster injection, the treatment groups received FAN (p.o.) while NOR and ART received saline, followed by behavioral assessments such as body weight measurement, arthritis index, paw edema measurement, and squeaking score. This was done every two days until day 43. The body weight was determined with the use of a digital scale and the arthritis index was measured to determine the severity of paw inflammation. Each paw was scored from 0 to 4, giving a total of 16 as the maximum arthritis index score for each mice. Each numerical score represented a corresponding condition which were as follows: 0=normal, 1=mild redness and swelling of one digit, 2=moderate redness and swelling of more than one digit or mild paw swelling, 3=severe redness with swelling of the entire paw and digits, 4=severe inflammation with ankylosing joints (Brand *et al*., 2007; Pietrosimone *et al*., 2015). Paw edema was measured by submerging the left and right hind limbs in the liquid with the use of a digital plethysmometer (Ugo Basile Biological Research Apparatus Company) and the mean of the two paws were used. The squeaking score was done in accordance to the method used in the C/K model stated above.

Histological assessment: On the last day of the experiments, the rats and mice were sacrificed and their knee joints were obtained. The knee joints underwent tissue processing to make paraffin blocks. The paraffin blocks were sectioned along the sagittal axis (5 μm; HistoCore multicut, Leica Biosystems, Wetzlar, Germany). Hematoxylin and eosin (H&E) staining was used to view the knee joint structure. Safranin-O staining is a special type of staining technique that was used to visualize cartilage in the tissue by staining the cartilage red. After staining the sections, it was mounted with a coverslip and were left to dry before analysis (Leica DM750, Leica Microsystems, Wetzlar, Germany). Scoring was done by three blinded independent researchers. Scoring for inflammation depended on the synovial membrane hyperplasia, extent of infiltration of immune cells, and the development of a pannus and increase of its size.

Statistical analysis: Prism 5.0 (GraphPad Software, San Diego, CA, USA) was used to graph and statistically analyze the data. Statistical analyses were conducted by using one-way ANOVA with Tukey's post-hoc testing and two-way ANOVA with Bonferroni's post-hoc testing. *p* values of <0.05 were considered to be statistically significant. All data are presented as means ± standard error of the means (SEM). The experiments were performed with duplicate samples for at least 3 times.

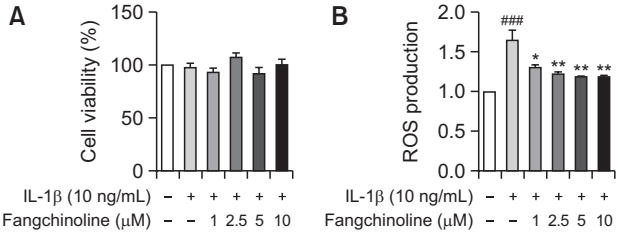

Fig. 2. Effect of fangchinoline on the cell viability and ROS production of IL-1β-stimulated human FLS cells. The cells were seeded and cultured using different doses of FAN (1, 2.5, 5, 10 μM). After 1 h, cells were then stimulated for 24 h with IL-1β, followed by WST-8 cell viability assay analysis (A) and H_2DCFDA-ROS production analysis (B), respectively. $^{###}p$<0.001 vs. untreated group; and $^{*}p$<0.05 and $^{**}p$<0.01 vs. only IL-1β-stimulated group (n=3).

RESULTS

Fangchinoline decreased the production of inflammatory mediators in IL-1β-stimulated human FLS cells

The WST-8 toxicity assay was used to determine if FAN has a cytotoxic effect on human FLS cells. The cell viability of human FLS cells after FAN treatment and 24 h IL-1β-stimulation was not significantly affected (Fig. 2A). Thus, the same concentrations were used for the subsequent assays. To look into the anti-inflammatory potential of FAN in synovial cells, ROS production of FAN-treated, IL-1β-stimulated human FLS cells was determined. After using H_2DCFDA to measure fluorescent intensity produced by ROS, FAN at different doses was found to have decreased ROS production significantly (Fig. 2B). To support the potential inhibitory effects of FAN on inflammation in stimulated human FLS cells, the protein expression levels of different inflammatory markers were acquired using western blot analysis (Fig. 3A, 3B). The protein expression of COX-2, IL-6, TNF-α, and iNOS were increased in human FLS cells stimulated with IL-1β. In contrast, these markers were found to have been significantly decreased by FAN. COX-2 and TNF-α protein levels decreased dose-dependently. At the same time, the IL-6 protein level decrease was significant at 10 μM and iNOS protein level decrease was significant at 5 and 10 μM. The consistent decrease of ROS and inflammatory markers in human FLS cells stimulated with IL-1β demonstrates the anti-inflammatory effect of FAN.

Fangchinoline inhibited the protein expression of MAPKs in human FLS cells stimulated with IL-1β

To explore the action of FAN on IL-1β-stimulated human FLS cells, the MAPK pathway was investigated. Phosphorylated MAPK protein expression was analyzed using western blot. The c-Jun N-terminal kinase (JNK), extracellular signal regulated kinase (ERK)1/2, and p38 total and phosphorylated forms were used in the analysis (Fig. 3C, 3D). JNK protein levels were decreased significantly on cells treated with 10 μM of FAN and FAN decreased the phosphorylation of p38 across all

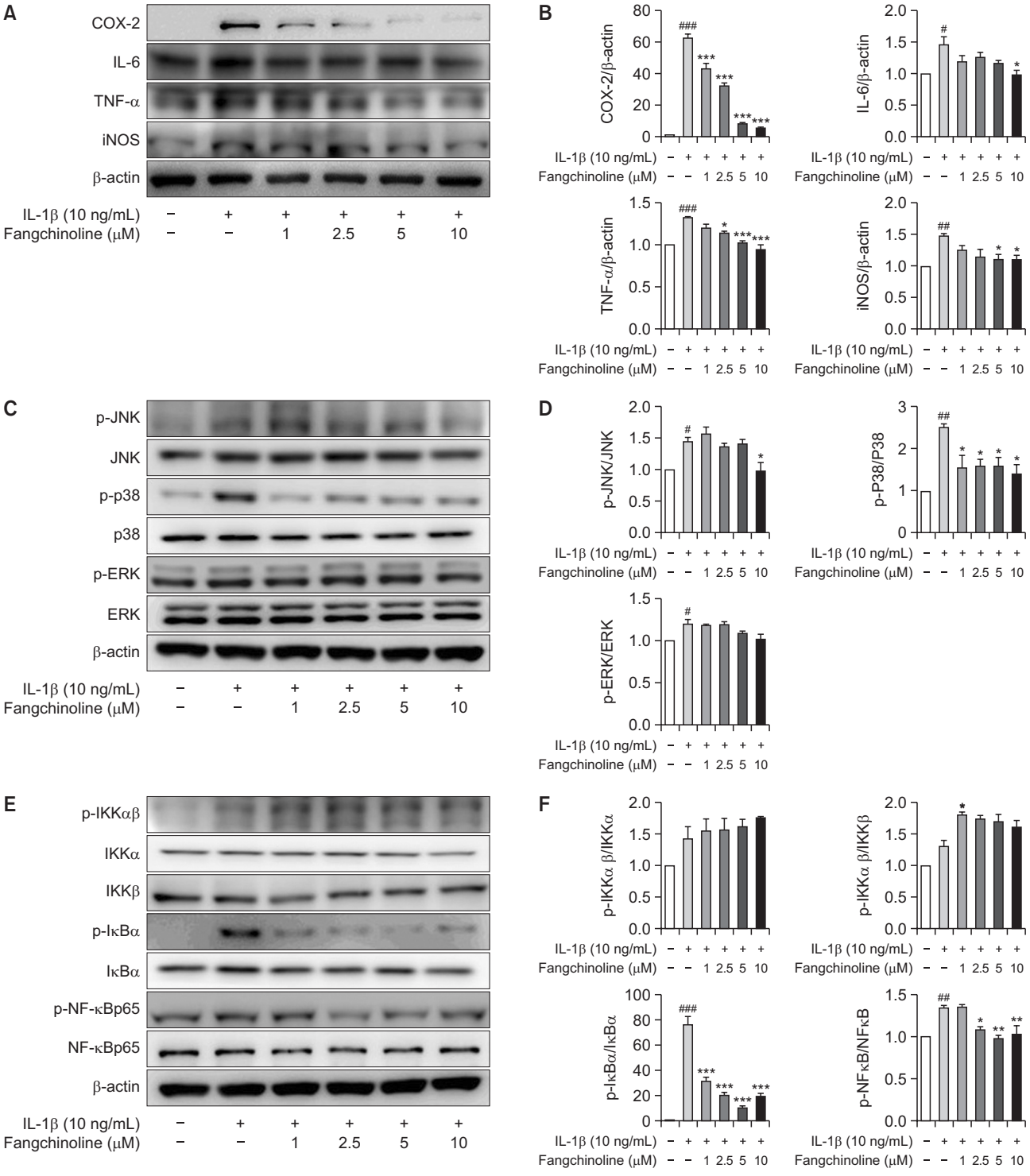

Fig. 3. Effects of fangchinoline on the expression of different inflammatory markers, MAPK, and NF-κB proteins on human FLS cells stimulated with IL-1β. Human FLS cells treated with FAN stimulated with IL-1β (10 ng/mL) western blot analysis of inflammatory mediators (A, B), MAPKs (C, D), and NF-κB (E, F). Fold induction of quantified western blot data. $^{\#}p<0.05$, $^{\#\#}p<0.001$, $^{\#\#\#}p<0.001$ vs. untreated group; and $^{*}p<0.05$, $^{**}p<0.01$, and $^{***}p<0.001$ vs. only IL-1β-stimulated group (n=3).

concentrations. However, FAN did not affect the phosphorylation of ERK in human FLS cells stimulated with IL-1β.

Fangchinoline inhibited the NF-κB protein expression in human FLS cells stimulated with IL-1β

To explore other possible actions of FAN on IL-1β-stimulated

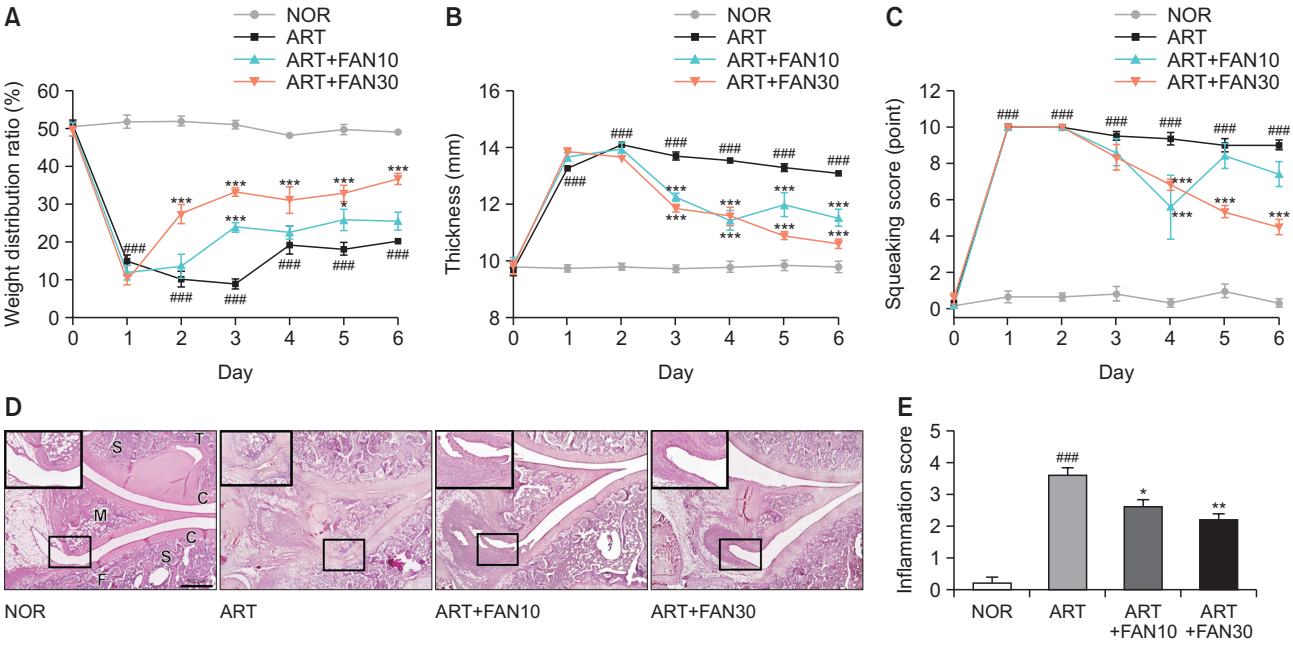

Fig. 4. Behavioral experiments and histological assessment of C/K arthritis rats and FAN treatment. Weight distribution ratio (A), knee thickness (B), and squeaking score (C) among all groups were used to compare arthritis severity (n=6). The paraffin sections were stained using H&E staining (×40) and the small black squares in the corner of each photo are magnified to ×100 (D). Inflammation score is presented in (E). Parts of the bone indicated are as follows: C: cartilage, F: femur, M: meniscus, S: subchondral bone, T: tibia. Scale bar is scaled to 500 μm. ###p<0.001 vs. NOR, *p<0.05, **p<0.01, and ***p<0.001 vs ART.

human FLS cells, the NF-κB pathway was investigated. The phosphorylation of NF-κB related proteins was measured using western blot analysis (Fig. 3E, 3F). FAN inhibited the phosphorylation of IκBα and NF-κB. FAN reduced the phosphorylation of IκBα significantly with all concentrations and NF-κB at 2.5, 5, and 10 μM. On the other hand, FAN did not have an effect on the phosphorylation of IKKαβ against IKKα and IKKβ.

Fangchinoline alleviated the severity of arthritic symptoms in C/K-induced arthritis rats

The efficacy of FAN on C/K-induced arthritis rats was investigated. Various parameters of arthritic symptoms were measured such as the squeaking score, knee thickness, and weight distribution ratio (WDR) (Fig. 4A-4C). Arthritic symptoms were evident in rats as early as the first day after C/K induction. A significant improvement in the arthritic symptoms was found in FAN30-treated rats. In all of the parameters, the arthritis group was found to be significantly different in comparison with the normal group. The left knee joints of rats were processed using histopathological techniques and hematoxylin and eosin (H&E) staining (Fig. 4D, 4E). FAN10 and FAN30-treated ratsboth showed a decrease in its inflammation score significantly compared to the ART group and is evident in the histological photos. Thus, the arthritic symptoms and pathological signs of inflammation in C/K arthritis was attenuated by FAN.

Fangchinoline alleviated the severity of arthritic symptoms in CIA mice

To further assess the efficacy of FAN as an anti-arthritic agent, a different arthritis animal model experiment was performed. The body weight, arthritis index, paw volume, and squeaking score were the four parameters measured to indicate arthritic symptoms in CIA mice (Fig. 5A-5D). After day 14, all four parameters started to become severe. The body weight of CIA FAN10-treated mice and FAN30-treated mice were found to have increasing body weight up to day 43. Even though this increase was not significant, it still shows improvement on the overall physical well-being of the FAN-treated mice. The arthritis index, paw volume, and squeaking score of ART was significantly increased until day 43 compared to the NOR group. The arthritis index was decreased significantly in mice treated with 10 and 30 mg/kg of FAN compared to the ART group. Both concentrations at 10 and 30 mg/kg had slow progression of arthritis. In both the paw volume and squeaking score, an increase was seen earlier in the FAN10 group compared to the FAN30 group. FAN30 developed the arthritic symptoms slower than the FAN10 group. The arthritic index, paw volume, and squeaking score for both FAN10 and FAN30 were all significantly decreased compared to the ART group on day 43. Paws of the mice on day 43 can be seen in Fig. 5E. The images show sustained arthritic signs and edema in the ART group while there is improvement on the paws of the mice treated with FAN. The knee joints of mice were processed and scored using the same techniques as mentioned in the C/K rats. The histopathological H&E staining images and inflammation score is shown in Fig. 5F and 5G. FAN10 and FAN30 both had a significant decreased inflammation score compared to the ART group. The knee joints of CIA mice were also stained using safranin-O in order to visualize the cartilage in the joints (Fig. 5H, 5I). FAN10 and FAN30 had a significant dose-dependent increase of stained cartilage area in comparison to ART. These observations show that FAN has

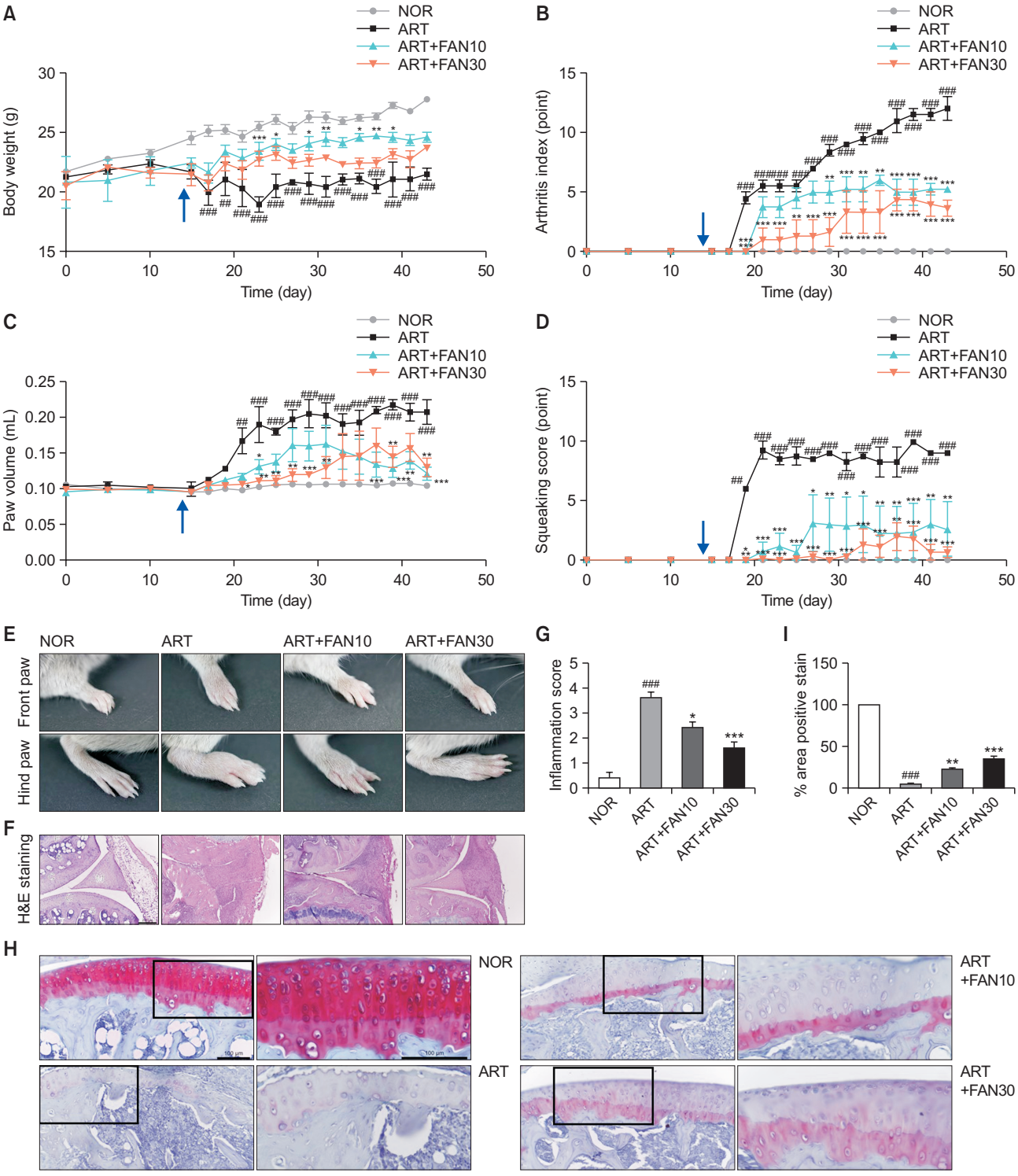

Fig. 5. Behavioral evaluation, paw images, and histological assessment of CIA mice and FAN treatment. Body weight (A), arthritis index (B), paw volume (C), and squeaking score (D) among all groups were used to compare the progression of arthritis in the groups. Arrows indicate day 14. Day 43 front and hind paws (E), H&E staining (F), and inflammation score (G) are indicated. Cartilage staining by Safranin-O is shown in (H) and (I). Parts of the bone indicated in photo are as follows: C: cartilage, F: femur, M: meniscus, S: subchondral bone, T: tibia. Scale bar is scaled to 200 μm. $^{\#\#}p<0.01$, $^{\#\#\#}p<0.001$ vs. NOR, and $^{*}p<0.05$, $^{**}p<0.01$, $^{***}p<0.001$ vs ART (n=6).

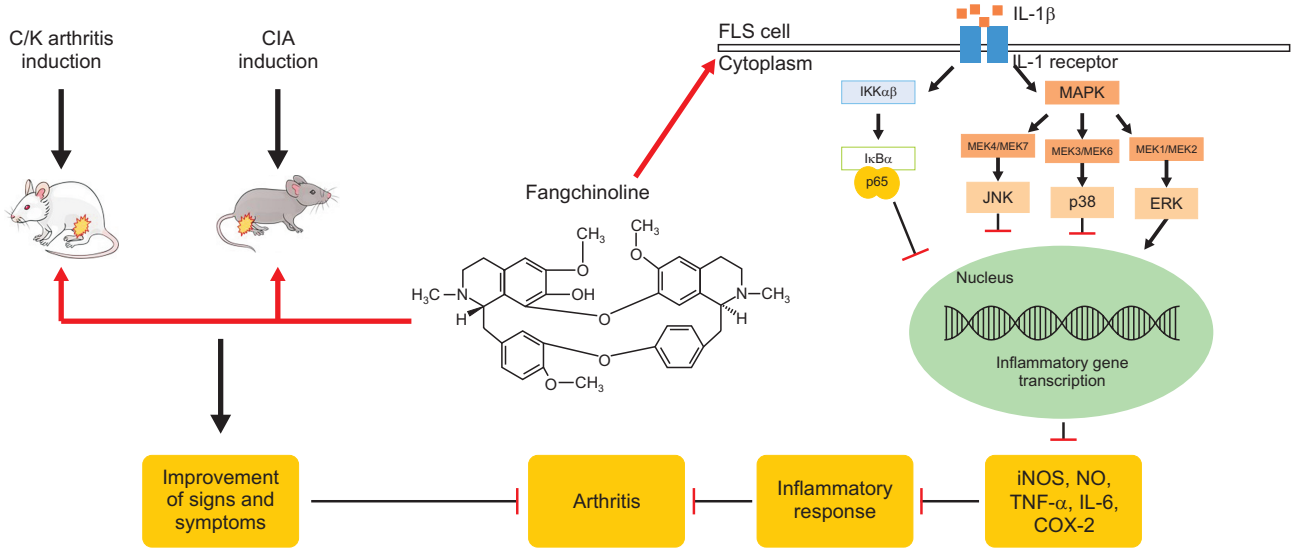

Fig. 6. Graphical model of FAN and its anti-arthritis effect in human FLS cells, C/K rat model, and CIA mice model. In the study, FAN attenuated arthritis by decreasing ROS production and pro-inflammatory cytokines through MAPK/NF-κB signaling. Anti-arthritic effect of FAN was also reflected in two animal models by decreasing arthritis severity in the joint and recovery of physical signs and symptoms.

an anti-arthritic effect on CIA mice.

DISCUSSION

Fangchinoline, a bisbenzylisoquinoline alkaloid, can be obtained from the roots of *Stephaniae tetrandra*. The compound has been mainly showed to have anti-cancer effects such as preventing the proliferation and metastasis of malignant cells as well as promoting autophagy and apoptosis in tumor cells (Mérarchi *et al*., 2018). However, there are hardly any studies involving FAN and arthritis.

Various arthritis animal models have been utilized in order to mimic RA in order to study its pathogenesis or for drug development. Such animal models include the C/K rat model and the CIA mouse model. In the C/K rat model, carrageenan acts as the arthrogenic compound while kaolin is the adjuvant that enhances the effectivity of carrageenan. Inducing arthritis using C/K will cause aseptic inflammation with manifestations of knee joint swelling, increased intra-synovial pressure in the joint, hyperthermia, and edema alongside increased cell infiltration. Physical manifestations of arthritis are evident through rodent pain behavior such as limping and decreased weight bearing on the affected knee (Neugebauer, 2013). Carrageenan can induce pro-inflammatory cytokine release including TNF-α, IL-1β, and IL-6 which results to formation of edema, immune cell migration, and promoting hypersentivity to pain (Annamalai and Thangam, 2017). Histological sections in carrageenan-induced arthritis have shown extensive damage of the articular cartilage of both the femur and tibia, large amount of inflammatory cells in the synovium, as well as proliferation and hypertrophy of the cells lining the synovium (Hansra *et al*., 2000). In the CIA mice model, collagen is used to induce arthritis alongside Freund's adjuvant to further stimulate the immune system. It is the most studied RA animal model and also displays RA-like features such as the presence of a hyperplastic synovium, immune cell infiltration, and cartilage destruction. In the CIA model, TNF-α and IL-1β are also present in mice joints. It goes without saying that inflammatory cytokines are a driving force in RA pathogenesis.

In RA, FLS cells have an important role to play. They produce various cytokines, proteases, and inflammatory mediators which contribute to joint destruction in RA (Burrage *et al*., 2006). FLS cells can also migrate, invade joint cartilage, and contribute to bone degradation (Fujiwara and Kobayashi, 2005; Bustamante *et al*., 2017). Inflammatory cytokines, such as TNF-α and IL-6, produced by FLS cells and macrophages drive the inflammation in RA. TNF-α mediates pro-inflammatory and bone-resorbing effects in RA, and IL-6 can also activate osteoclasts (Siouti and Andreakos, 2019). IL-1 and TNF can activate both synoviocytes and cytokines to produce cartilage-degrading enzymes and also upregulate other pro-inflammatory genes such as COX-2 and NOS which would result to increased PGE2 and NO. Furthermore, inflammation is sustained in RA as IL-1 and TNF upregulate each other (Kay and Calabrese, 2004). Thus, it is not surprising that inflammatory mediators and signaling pathways are one of the targets of current RA drug research (Aletaha and Smolen, 2018).

As the effects of FAN on human FLS cells, C/K rat model, and CIA mice model have not yet been studied, the purpose of this study was to investigate the inhibitory activity of FAN in arthritis using these models.

In the study, ROS production of human FLS cells after IL-1β stimulation was decreased dose-dependently by FAN. IL-1β stimulation of human FLS cells showed an increase protein expression in COX-2, IL-6, TNF-α, and iNOS. At the same time, the treatment of FAN on human FLS cells stimulated with IL-1β decreased the protein expression of the previously mentioned inflammatory mediators. Hence, FAN exhibits anti-arthritic activity as it can modulate human FLS cells that have been stimulated with IL-1β.

To investigate the biological actions as to how FAN exerts its anti-arthritic effects, western blot analysis on IL-1β-stimulated human FLS cells was done to examine the MAPK and NF-κB

pathways. The aforementioned are extensively being studied in the field of arthritis research, in particular p38 MAPK as it is considered to be a promising therapeutic target (Simmonds and Foxwell, 2008; Thalhamer *et al*., 2008). p38 MAPK and JNK MAPK phosphorylation were decreased by FAN significantly at 10 μM. In contrast, the phosphorylation of ERK was not affected by FAN. For the NF-κB pathway, FAN did not affect the phosphorylation of IKKαβ significantly. FAN also decreased IκBα phosphorylation and consequently, NF-κB phosphorylation. Thus, FAN decreases the IL-1β-stimulated human FLS cell inflammatory mediator production implicated in arthritis by impeding the MAPK and NF-κB pathway.

In the C/K model, the oral treatment of 10 and 30 mg/kg FAN on SD rats for 6 days attenuated the various behavioral parameters of arthritis in C/K rats. The weight distribution ratio, knee thickness, and squeaking score decreased consistently and significantly in rats treated with FAN especially for FAN30 rats. The decrease was most evident on the 6th day of the experiment. These indicate that the swelling of the synovial joint of the FAN-treated rats as well as the pain severity of the left-knee joint were reduced. The results of the behavioral parameters also paralleled the images from the H&E staining of the left knee joints. The histopathological analysis showed that there is decreased infiltration, decreased knee thickness, and decreased pannus formation. The behavioral symptoms and histopathological analysis showed improvement in FAN-treated arthritic rats dose-dependently suggesting that FAN has an anti-arthritic effect on C/K induced arthritis in rats.

The second animal arthritis model that was performed to further confirm the anti-arthritic effect of FAN was the CIA mice model. The four behavioral parameters that were evaluated were the body weight, arthritis index, paw volume, and squeaking score. Compared to the ART group, the body weight of the FAN-treated mice was not statistically significant on the last day but still showed a decrease indicating an improvement in their metabolism brought upon by FAN treatment. The arthritis index, which measures the appearance of inflammatory signs in the paws of the mice, was also decreased in the FAN-treated groups dose-dependently. The paw volume and squeaking scores were significantly decreased in both the FAN10 and FAN30 groups compared to the arthritis mice. It was observed that in the evaluation of the behavioral parameters in arthritis that the FAN30 mice had reduced symptoms of arthritis and slower disease progression in comparison to FAN10 mice. H&E evaluation indicated that there is decreased pannus formation, synovial hyperplasia, and immune cell infiltration. Safranin-O staining also revealed that there is less cartilage degradation in the knee joints of the FAN30 group in comparison to the ART group. The histopathological results are in accordance with the results in the behavioral assessment. Hence, FAN showed an anti-arthritic effect on CIA mice.

We have explored the anti-arthritic effects of FAN in human FLS cells and two animal models in this study. It was found that FAN can exhibit these effects possibly through the MAPK and NF-κB pathway. Even though the exact mechanisms and target receptors as to how FAN can modulate these effects have yet to be elucidated, this study highlights how FAN can demonstrate its anti-arthritic effects and provide support for FAN as a potential therapeutic agent for arthritis.

ACKNOWLEDGMENTS

This research was supported by a National Research Foundation (NRF) grant funded by the Korean Ministry of Science, ICT & Future Planning (MRC 2010-0029355).

REFERENCES

Aletaha, D. and Smolen, J. S. (2018) Diagnosis and management of rheumatoid arthritis: a review. *JAMA* **320**, 1360-1372.

Annamalai, P. and Thangam, E. B. (2017) Local and systemic profiles of inflammatory cytokines in carrageenan-induced paw inflammation in rats. *Immunol. Invest.* **46**, 274-283.

Bao, F., Tao, L. and Zhang, H. (2019) Neuroprotective effect of natural alkaloid fangchinoline against oxidative glutamate toxicity: involvement of keap1-Nrf2 axis regulation. *Cell. Mol. Neurobiol.* **39**, 1177-1186.

Brand, D. D., Latham, K. A. and Rosloniec, E. F. (2007) Collagen-induced arthritis. *Nat. Protoc.* **2**, 1269-1275.

Burrage, P. S., Mix, K. S. and Brinckerhoff, C. E. (2006) Matrix metalloproteinases: role in arthritis. *Front. Biosci.* **11**, 529-543.

Bustamante, M. F., Garcia-Carbonell, R., Whisenant, K. D. and Guma, M. (2017) Fibroblast-like synoviocyte metabolism in the pathogenesis of rheumatoid arthritis. *Arthritis Res. Ther.* **19**, 1-12.

Choi, H. S., Kim, H. S., Min, K. R., Kim, Y., Lim, H. K., Chang, Y. K. and Chung, M. W. (2000) Anti-inflammatory effects of fangchinoline and tetrandrine. *J. Ethnopharmacol.* **69**, 173-179.

Fujiwara, N. and Kobayashi, K. (2005) Macrophages in inflammation. *Curr. Drug Targets Inflamm. Allergy* **4**, 281-286.

Hansra, P., Moran, E. L., Fornasier, V. L. and Bogoch, E. R. (2000) Carrageenan-induced arthritis in the rat. *Inflammation* **24**, 141-155.

Heidari, B. (2011) Rheumatoid arthritis: early diagnosis and treatment outcomes. *Caspian J. Intern. Med.* **2**, 161-170.

Hristova, M., Yordanov, M. and Ivanovska, N. (2003) Effect of fangchinoline in murine models of multiple organ dysfunction syndrome and septic shock. *Inflamm. Res.* **52**, 1-7.

Jiang, Y., Liu, J., Zhou, Z., Liu, K. and Liu, C. (2018) Fangchinoline protects against renal injury in diabetic nephropathy by modulating the MAPK signaling pathway. *Exp. Clin. Endocrinol. Diabetes* **126**, 1-7.

Kay, J. and Calabrese, L. (2004) The role of interleukin-1 in the pathogenesis of rheumatoid arthritis. *Rheumatology (Oxford)* **43 Suppl 3**, iii2-iii9.

Li, X., Yang, Z., Han, W., Lu, X., Jin, S., Yang, W., Li, J., He, W. and Qian, Y. (2017) Fangchinoline suppresses the proliferation, invasion and tumorigenesis of human osteosarcoma cells through the inhibition of PI3K and downstream signaling pathways. *Int. J. Mol. Med.* **40**, 311-318.

Mérarchi, M., Sethi, G., Fan, L., Mishra, S., Arfuso, F. and Ahn, K. S. (2018) Molecular targets modulated by fangchinoline in tumor cells and preclinical models. *Molecules* **23**, 2538.

Müller-Ladner, U., Pap, T., Gay, R. E., Neidhart, M. and Gay, S. (2005) Mechanisms of disease: the molecular and cellular basis of joint destruction in rheumatoid arthritis. *Nat. Clin. Pract. Rheumatol.* **1**, 102-110.

Neugebauer, V. (2013) Arthritis model, kaolin-carrageenan-inducedarthritis (knee). In Encyclopedia of Pain, 2nd ed. (G. F. Gebhart and R. F. Schmidt, Eds.), pp. 190-195. Springer, Heidelberg.

Pietrosimone, K., Jin, M., Poston, B. and Liu, P. (2015) Collagen-induced arthritis: a model for murine autoimmune arthritis. *Bio Protoc.* **5**, e1626.

Schett, G., Tohidast-Akrad, M., Smolen, J. S., Schmid, B. J., Steiner, C. W., Bitzan, P., Zenz, P., Redlich, K., Xu, Q. and Steiner, G. (2000) Activation, differential localization, and regulation of the stress-activated protein kinases, extracellular signal-regulated kinase, c-Jun N-terminal kinase, and p38 mitogen-activated protein kinase, in synovial tissue and cells in rheumatoid arthritis. *Arthritis Rheum.* **43**, 2501-2512.

Shan, L., Tong, L., Hang, L. and Fan, H. (2019) Fangchinoline supplementation attenuates inflammatory markers in experimental

rheumatoid arthritis-induced rats. *Biomed. Pharmacother.* **111**, 142-150.
Simmonds, R. E. and Foxwell, B. M. (2008) Signalling, inflammation and arthritis: NF-κB and its relevance to arthritis and inflammation. *Rheumatology* **47**, 584-590.
Siouti, E. and Andreakos, E. (2019) The many facets of macrophages in rheumatoid arthritis. *Biochem. Pharmacol.* **165**, 152-169.
Thalhamer, T., McGrath, M. A. and Harnett, M. M. (2008) MAPKs and their relevance to arthritis and inflammation. *Rheumatology* **47**, 409-414.
Wang, B., Xing, Z., Wang, F., Yuan, X. and Zhang, Y. (2017) Fangchinoline inhibits migration and causes apoptosis of human breast cancer MDA-MB-231 cells. *Oncol. Lett.* **14**, 5307-5312.